PSFC/JA-09-40

Rotation and Transport in Alcator C-Mod ITB Plasmas

C. L. Fiore, J. E. Rice, Y. Podpaly,
I. O. Bespamyatnov[†], W. L. Rowan[†],
J.W. Hughes, M. Reinke

[†]FRC, U of Texas at Austin, Austin, TX 78712, USA;
w.l.rowan@mail.utexas.edu

May 2010

Plasma Science and Fusion Center
Massachusetts Institute of Technology
Cambridge MA 02139 USA

This work was supported by the U.S. Department of Energy, Grant No. US-DOE DE-FC02-99ER54512 and DE-FG03-96ER54373.

Nuclear Fusion 12th International H-Mode Workshop Special Issue

Rotation and Transport in Alcator C-Mod ITB Plasmas

C. L. Fiore*, J. E. Rice*, Y. Podpaly*, I. O. Bespamyatnov†, W. L. Rowan†, J.W. Hughes*, M. Reinke*

* MIT-PSFC, 77 Mass. Ave., Cambridge, MA 02139, USA; fiore@psfc.mit.edu

†FRC, U of Texas at Austin, Austin, TX 78712, USA; w.l.rowan@mail.utexas.edu

Catherine L. Fiore

MIT Room NW21-203

77 Mass. Ave.

Cambridge, MA 02139

617-253-8440

617-252-1808 (Fax)

fiore@psfc.mit.edu

19 pages including this cover sheet

13 figures

Rotation and Transport in Alcator C-Mod ITB Plasmas

C. L. Fiore[*], J. E. Rice[*], Y. Podpaly[*], I. O. Bespamyatnov[†], W. L. Rowan[†], J.W. Hughes[*], M. Reinke[*]

[*] MIT-PSFC, 77 Mass. Ave., Cambridge, MA 02139, USA; fiore@psfc.mit.edu

,[†]FRC-UTA, U of Texas at Austin, Austin, TX 78712, USA; w.l.rowan@mail.utexas.edu

Abstract

Internal transport barriers (ITBs) are seen under a number of conditions in Alcator C-Mod plasmas. Most typically, radio frequency power in the ion cyclotron range of frequencies (ICRF) is injected with the second harmonic of the resonant frequency for minority hydrogen ions positioned off-axis at r/a > 0.5 to initiate the ITBs. They also can arise spontaneously in ohmic H-mode plasmas. These ITBs typically persist tens of energy confinement times until the plasma terminates in radiative collapse or a disruption occurs. All C-Mod core barriers exhibit strongly peaked density and pressure profiles, static or peaking temperature profiles, peaking impurity density profiles, and thermal transport coefficients that approach neoclassical values in the core. The strongly co-current intrinsic central plasma rotation that is observed following the H-mode transition has a profile that is peaked in the center of the plasma and decreases towards the edge if the ICRF power deposition is in the plasma center. When the ICRF resonance is placed off-axis , the rotation develops a well in the core region. The central rotation continues to decrease as long as the central density peaks when an ITB develops. This rotation profile is flat in the center($0<r/a<0.4$) but rises steeply in the region where the foot in the ITB density profile is observed ($0.5<r/a<0.7$). A correspondingly strong EXB shear is seen at the location of the ITB foot that is sufficiently large to stabilize ion temperature gradient (ITG) instabilities that dominate transport in C-Mod high density plasmas.

Work supported by US-DoE DE-FC02-99ER54512 and DE-FG03-96ER54373

I. *Introduction*

Transport barriers that provide regions of reduced energy, particle, and/or momentum transport have been observed in a large number of toroidal plasma experiments. The edge transport barrier which gives rise to the enhanced confinement regime known as H-mode[1] is ubiquitous in toroidal plasmas and forms the benchmark for optimized plasma performance. Transport barriers often occur in the plasma interior as well, usually under very specific operational conditions. Most commonly, transport barriers in the plasma interior are found in neutral beam heated plasmas [2,3,4,5,6] where the beam provides a source of particles, momentum and energy to the plasma. The neutral beam induced rotation of the plasma generates sufficient electromagnetic shear to stabilize ion temperature gradient driven instability (ITG) by increasing the E X B shearing rate above its maximum linear growth rate, as has been observed in numerous experiments [7,8,9,10,11]. Indeed, the relationship between observed rotation and thermal transport has been studied in L-mode plasmas with spontaneous rotation[12,13], in L-and H-mode plasmas that evolve intrinsic rotation with ion cyclotron range of frequency (ICRF) heating [14], with low torque injection (balanced neutral beams)[9,15], and with electron cyclotron heating[16,17]. Other techniques use radio frequency waves to alter the internal magnetic configuration of the plasma to obtain magnetic shear stabilization of microturbulence. These include lower hybrid current drive[18,19], electron cyclotron heating[20], and ion Bernstein wave injection[21].. A comprehensive review of the internal transport barrier experiments and analysis can be found in papers by Wolf[22] and Connor[23].

The Alcator C-Mod experiment provides a unique platform in the study of internal transport barrier physics in several aspects. The sole source of heating to the plasma other

than from the ohmic current is provided by up to 8 MW of balanced ICRF power. Thus there is neither momentum input nor particle input into the plasma. The observed rotation is entirely intrinsic in origin [14]. The C-Mod target plasmas used for these studies are very high density, typically 1 x $10^{20}/m^3$ before the ITB is induced, and the ions and electrons are thermally equilibrated. The q-profile is monotonic with q_{min} less than one at the center, as evidenced by sawtoothing activity before and during ITB development[24].

Internal transport barriers induced by off-axis ICRF heating in Alcator C-Mod were first reported by Rice *et al.* in 2001[25], and it was noted then that a significant slowing of the intrinsic central rotation occurred in concert with the ITB development. Gyrokinetic modeling of C-Mod plasmas demonstrates that the ITG mode fluctuations dominate the particle diffusion in the target plasmas used for ITB studies[26]. The ion temperature and rotation measurements available prior to 2007 lacked sufficient temporal and spatial resolution to resolve whether the change in the toroidal angular momentum was a cause or a result of the ITB formation. Subsequent experimental and gyrokinetic examination of the onset conditions for ITB development in Alcator C-Mod sought to answer this question. Redi[27] concluded that the ion temperature profile that occurs with off-axis heating is broad enough to reduce the ITG drive term that dominates the transport in these high density plasmas. The work of Zhurovich *et al.* [28] supported this conclusion and demonstrated how the change in ICRF resonance position affects the ion temperature profiles and resulting turbulence driven flux. Zhurovich was also able to demonstrate with the gyrokinetic modeling that the small magnetic shear found in the core region of Alcator C-Mod was not significant in suppressing the ITG instability in these plasmas. Neither of these studies incorporated rotational shear in the analysis because of code limitations and lack of detailed experimental profiles.

In this paper we present the results obtained with two new rotation diagnostics that were not available in the earlier experimental studies in Alcator C-Mod ITB plasmas. The

combination of these diagnostics provides radial profiles across the plasma. Improvement in the temporal sampling of the data allows examination of the cause and effect of rotation on ITB formation in this device.

II. *Alcator C-Mod ITBs*

In C-Mod plasmas (R=0.69 m, a=0.21 m) where an enhanced D_α H-mode (EDA) is established in which the net central power is not peaked on axis (as when the ICRF resonance is placed at the half radius on either the low or high field side of the plasma), a long-lived ITB usually arises. ICRF heating in Alcator C-Mod uses a fixed frequency so the resonance position is changed by adjusting the toroidal magnetic field value. All of the ITBs presented in this paper were obtained with 80 Mhz ICRF, with either high field side resonance ($B_{toroidal} \leq 4.5$ T) or low field sided resonance ($B_{toroidal} \geq 6.2$ T). The centrally heated H-mode discharges use $B_{toroidal}=5.4$T. Typical ITBs have been observed to last 10 or more confinement times. They are most notable in that the plasma density profile becomes very strongly peaked, and often displays a distinctive break in the profile near the plasma half radius. The break in slope (referred to as the ITB foot) is particularly evident in profiles of the square root of the visible bremsstrahlung radiation[29] which has been corrected for the small contribution of $T_e^{-1/2}$ leaving $V_b = n_e^2 * Z_{eff}$. Z_{eff} is the average charge state of the plasma and is between 1 and 2 for most Alcator C-Mod plasmas and has been demonstrated to be flat across the plasma profile when the data is compared with the density measured with Thomson scattering[30], $Z_{eff}=\sqrt{V_b}/n_e$. The exception occurs late in the life of an ITB when some impurities begin to accumulate in the core, often triggering a disruption or a collapse of the H-mode. The peaking of the density indicates that a strong barrier to particle transport has formed. The pressure profile also displays strong gradients. This implies that no loss in thermal energy is occurring as the core density rises and indicates that a thermal barrier exists

in the plasma interior as well. Details of prior experimental and modeling analysis of Alcator C-Mod ITBs are summarized in a recent review paper[31]

An example of a typical ITB density profile obtained from Thomson scattering is shown in Fig. 1.a The ICRF resonance in this case was located at r/a=0.5. While the ITB foot is found near the ICRF resonance, its location does not correlate well with the position of the ICRF power deposition. Instead, it has been shown that it moves inversely with q_{95}, and corresponds most closely to the location of q=4/3[32].

The electron pressure profile obtained from Thomson scattering data is presented in figure 1b. The pressure profile becomes quite peaked after the onset of the ITB emphasizing that there is no decline in the temperature in the core despite the strong increase in the density.

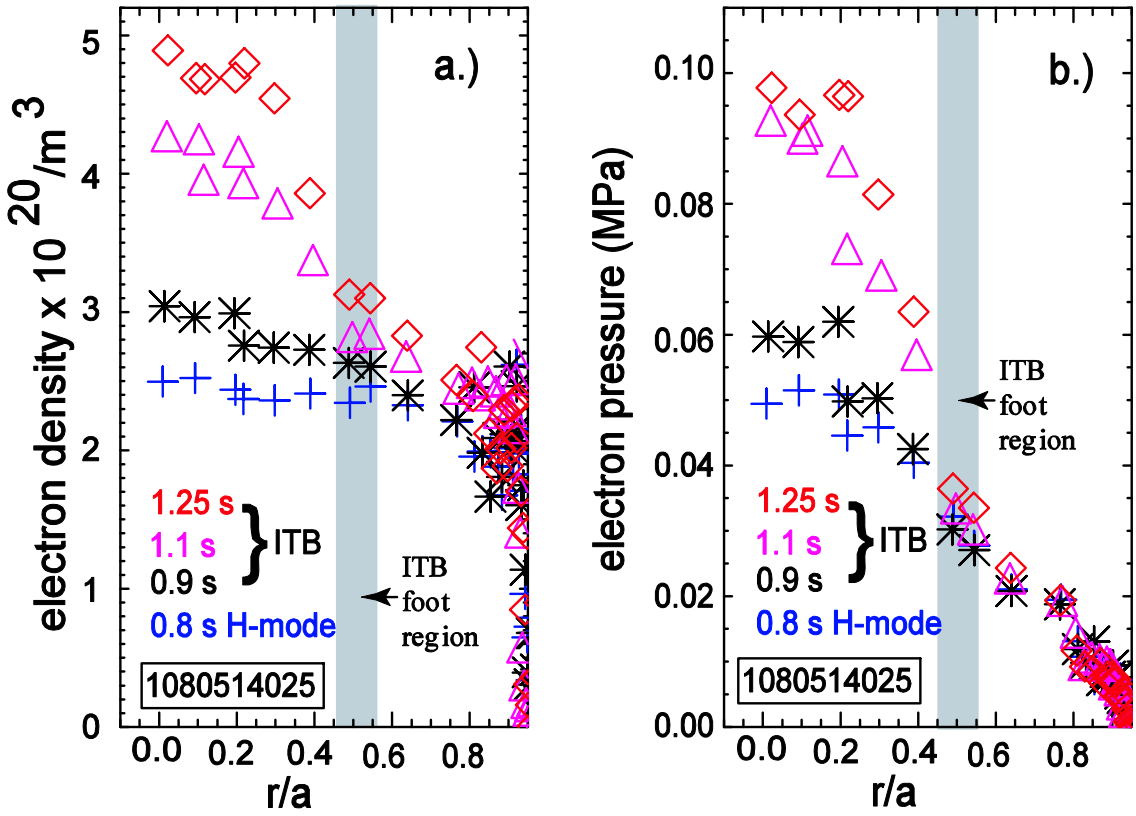

Fig 1 a.) Density profile in C-Mod ITB plasma with off-axis ICRF heating as the profile peaks from H-mode (blue +) to ITB development (black *) to ITB established (violet Δ and red ◊). b.)The pressure profile from Thomson scattering shortly after the H-mode transition

(blue +), during ITB start (black *) and during the ITB (magenta Δ and red ◊). The region where the ITB foot occurs is shaded.

Ion and electron temperatures, shown in Fig. 2, are not as dramatically peaked as the density profiles during the ITB phase of the plasma, but they do show a change in the slope in the region of the ITB foot. The ion temperature profiles are derived from the broadening of argon and molybdenum lines recorded by an array of von Hamos type x-ray crystal spectrometers[33] and an imaging Johann x-ray spectrometer system (HIREX) [34]. The electron temperature profiles are from Thomson scattering, and the central T_i is obtained by inverting the global neutron rate using the Thomson electron density profiles.

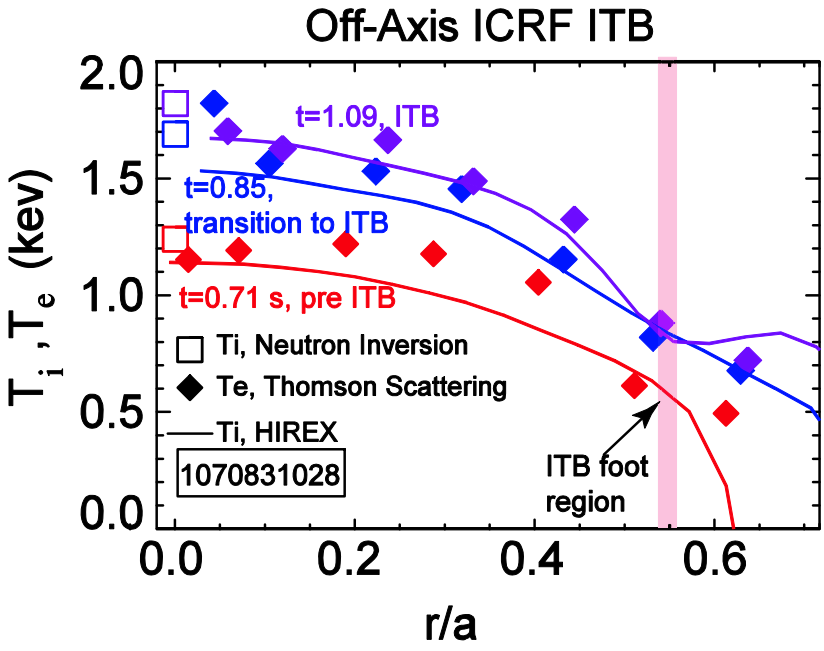

Fig. 2. Ion and electron temperature profiles during an ITB plasma. T_i from x-ray emission (solid lines), before ITB (red), at transition (blue) and as established (purple); T_e from Thomson scattering at the corresponding times (diamonds); and central T_i from neutrons (squares). The ITB foot location is marked by the band.

Light impurity ions such as B^{+5} peak in the plasma center as the ITB develops, as do the heavier impurity ions [35], which show even stronger peaking. Data obtained from charge exchange recombination spectroscopy aided by a diagnostic neutral beam are shown in Fig.

3a. Initially the boron profile (B^{+5} is the only boron species present at r/a < 0.7) peaks off axis at the H-mode transition. As the central density rises in the ITB phase, the B^{+5} profile fills in and then, becomes very peaked in the later stage of the ITB. The electron density profiles are included for comparison.

The particle flux is represented by $\Gamma = -D\,\frac{\partial n_z}{\partial r} + \mathrm{v}\, n_z$ where D is the diffusion coefficient and v represents the off-diagonal terms in the transport matrix. In this case, only the ratio v/D can be extracted from the data since v cannot be separated from D in the absence of perturbative experiments. Interpreting the inverse scale length of the impurity profile to represent the ratio of convection to diffusion, allows the inference that a strong impurity pinch occurs in the range of 0.1 < r < 0.4 (shaded region) is shown in Fig. 3.b [36]. The pinch profile used to simulate the measurements used a boundary condition of v=0 at r/a =0 and was optimized for the shaded region. Thus the plot is not extended to r/a=0.

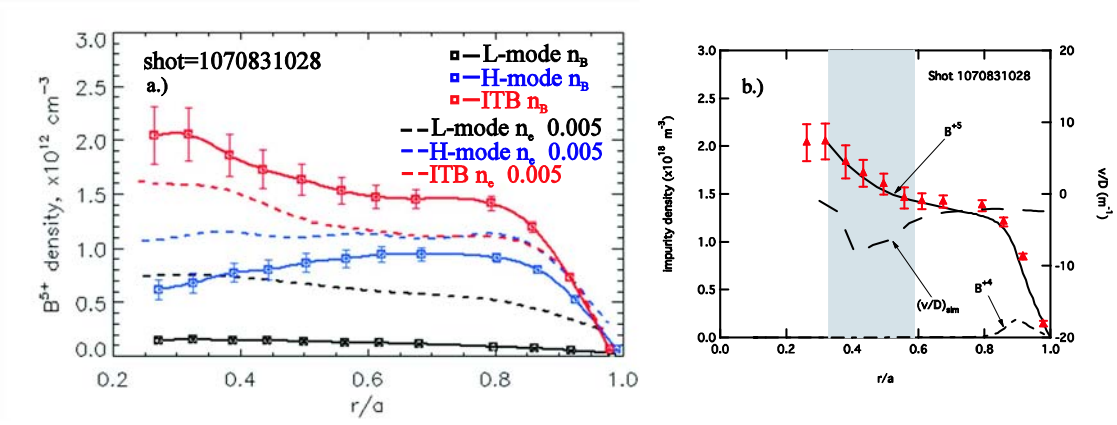

Fig. 3. a.) The B^{+5} profiles as measured with CXRS (squares ,solid lines) at 3 temporal points in the discharge: black, L-mode, blue,H-mode, red, ITB are compared with the electron density (dashed lines) at the same times. b.) The pinch term v/D (dashed line) used to model the boron profile during the ITB (solid line) shown with the data (triangles).

III. *Plasma Rotation in Alcator C-Mod ITBs*

Alcator C-Mod H-mode plasmas demonstrate strong co-going central plasma rotation that switches from the counter direction typical of L-mode plasmas following the H-mode

transition. An example is shown in Fig. 4. Both the central rotation and that found just beyond the half radius in a typical EDA H-mode with the ICRF resonance on axis are shown. The large positive toroidal rotation found in the center is in stark contrast to the behavior of the rotation when an ITB develops, as is seen in Fig. 5. The counter-going rotation in the L-mode becomes co-going after the H-mode transition, then decreases in the center becoming more strongly counter as the ITB develops. The change in the velocity trend occurs before any peaking in the density can be seen from the ITB.

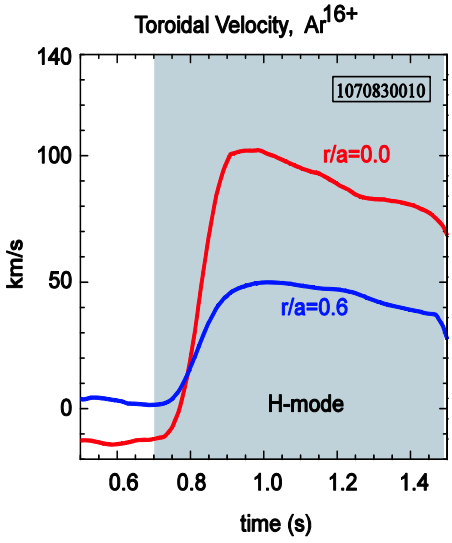

Fig. 4 The toroidal rotation as a function of time for r/a=0 (red) and r/a=0.6 (blue) for a centrally ICRF heated EDA H-mode plasma. There was no ITB in this plasma.

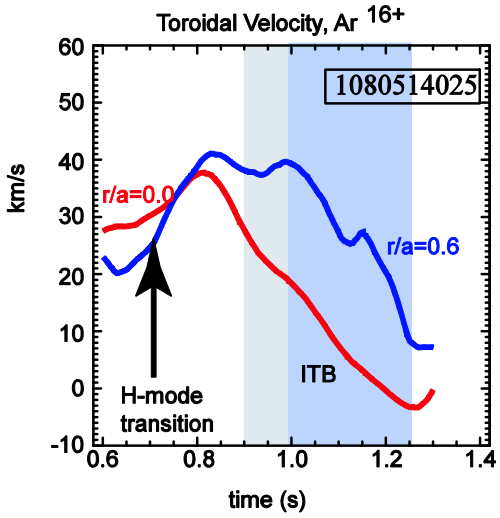

Fig. 5. The toroidal rotation as a function of time for r/a=0 (red) and r/a=0.6 (blue) for an off-axis ICRF heated EDA H-mode plasma that developed an ITB. The ITB onset time is shaded in grey, and the established ITB persists through the blue shaded time.

The rotation radial profile during an H-mode plasma with central ICRF heating is peaked on axis and remains so throughout the H-mode (Fig. 6). In contrast, with ICRF injected off-axis, the rotation profile is peaked at r/a>0.6 As the ITB develops, the rotation velocity in the core (0 <r/a<0.5) becomes more negative and displays a deepening well in the center of the plasma. As the density continues to peak with increasing time, the value becomes even lower, deepening the core well as can be seen in Fig. 7.

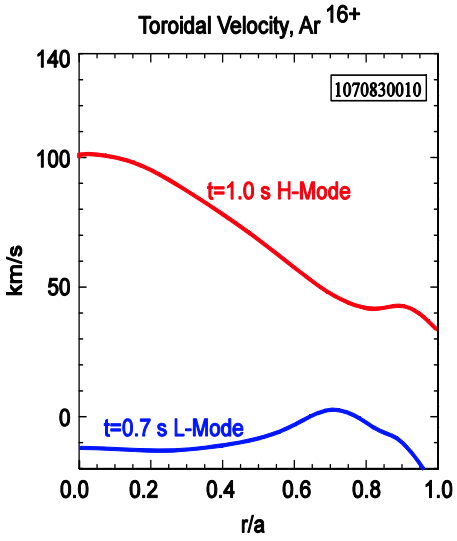

Fig. 6 The radial profile of the toroidal during L-mode (blue) and H-mode (red) for a centrally ICRF heated EDA H-mode plasma,TRANSP-NCLASS calculation using experimental toroidal rotation data from 0 <r/a<0/7. There was no ITB in this plasma.

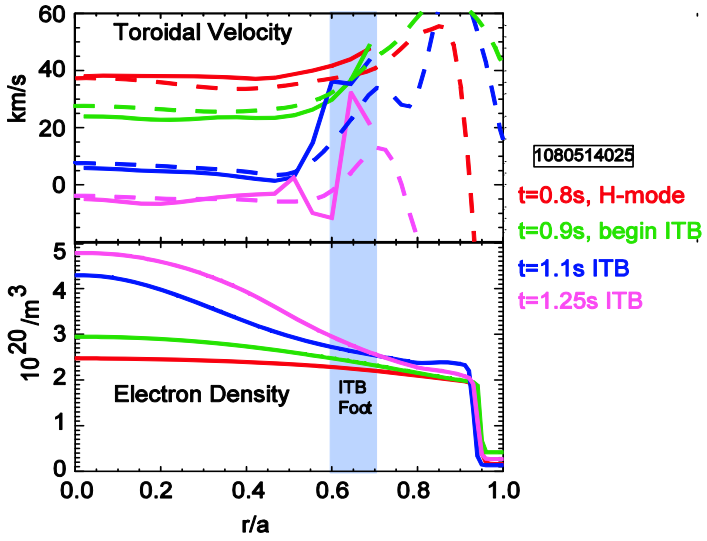

Fig. 7 Toroidal velocity profile at 4 times in the development of an ITB compared with the electron density profile: following the H-mode transition (red), beginning of peaking for the ITB (green), established ITB (blue), just prior to the back transition (violet). Solid lines are measured profiles. Dashed lines are smoothed profiles output from TRANSP/NCLASS using experimental data from 0<r/a<0.7.

The radial profile following the H-mode transition that is seen in Fig. 7 is characteristic of plasmas with off-axis ICRF heating even if no ITB forms. An initial decline

in the core rotation is seen in off-axis heated discharges that do not develop an ITB. However, the core rotation reaches its final value by t=1.0 s a deep well in the rotation profile such as that of Fig. 7 is not seen for non-ITB off-axis heated H-mode plasmas.

IV. *Electric Field and EXB shear in Alcator C-Mod ITBs*

The measured toroidal velocity profile, in this case obtained from Doppler shifted $_{40}Ar^{16+}$ impurities, is used as an input to the transport code TRANSP [37]. TRANSP incorporates the general geometry neoclassical code NCLASS [38] to determine the rotation profiles of all remaining plasma species and to derive the neoclassical radial electric field.

The total radial electric field for a centrally heated H-mode plasma as a function of radius is displayed in Fig. 8.a. In addition, the components of the radial electric field from the plasma pressure, the toroidal rotation, and the calculated poloidal rotation are displayed as well. The toroidal rotation component forms the largest contribution to the radial electric field E_r. E_r reaches a maximum value of 50 kV/m at r/a ~ 0.45. In contrast, in an off-axis ICRF heated discharge in which and ITB has developed, the radial electric field exhibits a well (Fig. 8.b). Again the component from the toroidal rotation makes up the dominant contribution to the radial electric field. Once the ITB is established E_r in is near zero at the center and rises to a value of 20 kV/m in the ITB region.

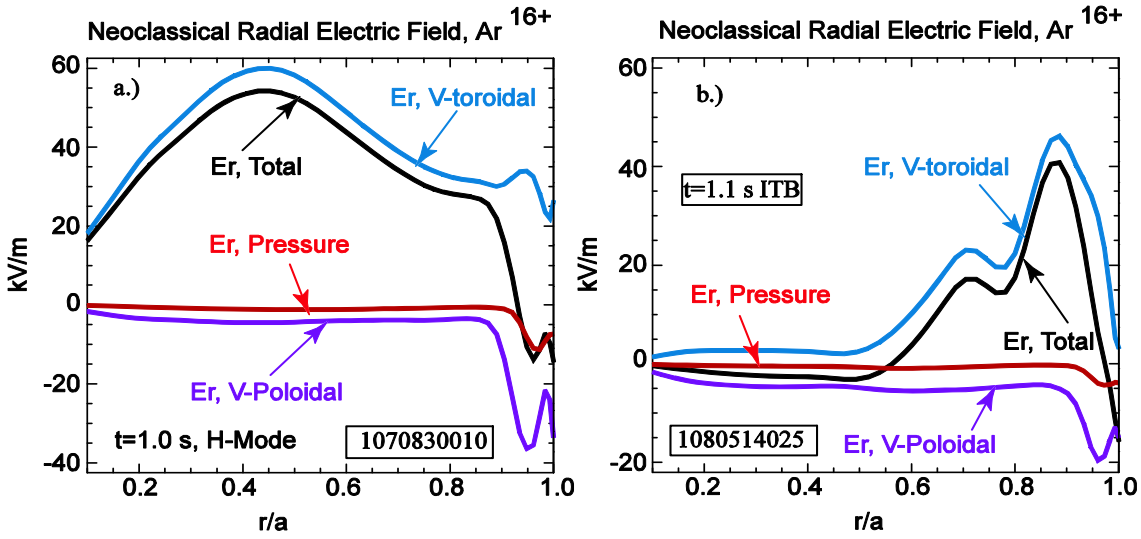

Fig. 8. The components of the radial electric field for a.) centrally ICRF heated EDA H-mode plasma and b.) off-axis ICRF heated EDA H-mode plasma with an ITB; total radial electric field (black), pressure term (red), poloidal velocity term (purple), toroidal rotation term (blue).

It was discussed in the previous section that the rotation profile in an off-axis ICRF heated discharge is similar to the case that did not form an ITB. Thus the electric field is expected to show similar profiles in both of the off-axis heated plasmas when compared to that with central heating. The radial electric fields calculated for an ITB case and from a non-ITB off-axis heated case both rise from the center to an off-axis peak of up to 40 kV/m following the H-mode transition (Fig. 9). However, in the ITB case the core rotation decreases towards zero as the ITB develops. What is significant here is the gradient in the electric field between $0.4<r/a<0.8$ The electric field is steeper going outward in the case that formed an ITB indicating higher E X B shearing rate in the outer half of the plasma that could promote the ITB formation.

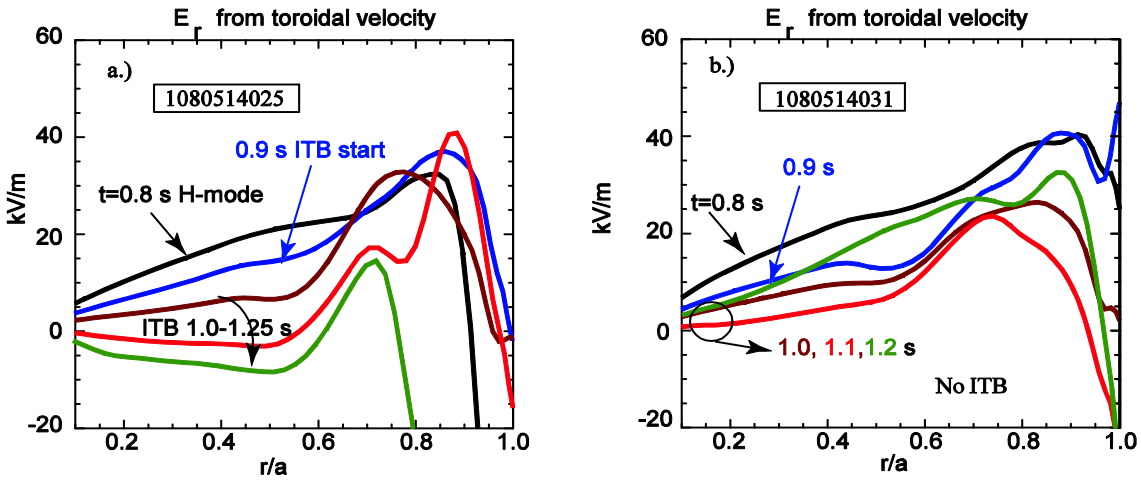

Fig. 9 Total radial electric field at several times for two off-axis ICRF heated EDA H-mode plasmas a.) with an ITB and b.) no ITB. Just after H-mode transition (black), and as the ITB evolves in a.) (blue, brown, red, green) and the corresponding times without ITB in b.)

The EXB shearing rate is displayed in Fig 10.a. for the standard centrally ICRF heated H-mode plasma. The shearing rates is twice as high during the H-mode than during the L-mode phase of the plasma although the maximum value remains low, less than 0.8 x 10^5 radians/sec. It is broadly peaked at the plasma half radius. During an off-axis heated ICRF discharge in which an ITB develops, the EXB shearing rate is significantly stronger, reaching a value of 1.5 x 10^5 radians/sec outside of the plasma half radius (Fig. 10.b.) It should be noted that the ITB foot in this plasma was located at $0.6 < r/a < 0.7$, which is the region of highest shearing rate. The case in which off-axis ICRF heating was used to obtain an H-mode that failed to form an ITB is included in Fig. 10.c. The radial profile of the shearing rate shown in 10c is similar to that of the ITB discharge in 10 b, but the magnitude is smaller and it does not exceed 1 x 10^5 radians/sec.

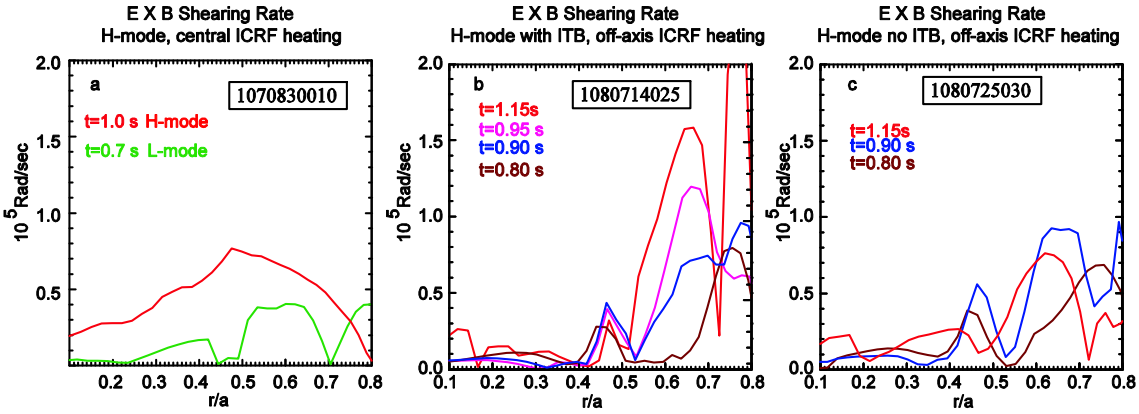

Fig. 10. EXB shearing rate for a.) centrally ICRF heated EDA H-mode plasma during L-mode (green) and H-mode (red), b.) off axis ICRF heated EDA H-mode plasma with ITB after H-mode transition (brown), ITB start (blue), ITB growth (violet), ITB established (red), and c.) off axis ICRF heated EDA H-mode plasma with no ITB after H-mode transition (brown) and at times corresponding to those in b,)

The time history of the EXB shearing rate increase in the ITB case is illustrative. The shearing rate is increases outside of the half radius following the H-mode transition (Fig 11.a.) The increase in shearing rate is evident at t=0.87 s in the plasma with an ITB, yet the peaking of the density profile characteristic of C-Mod ITBs is not obvious until t > 1.0 s (Fig 11.b). The case in which an ITB developed reaches a 50% to 80% higher value of shearing rate than in non-ITB cases. It increases most strongly at r/a=0.6, the ITB foot region, No change in the shearing rate is seen further into the interior of the plasma, r/a <0.5.

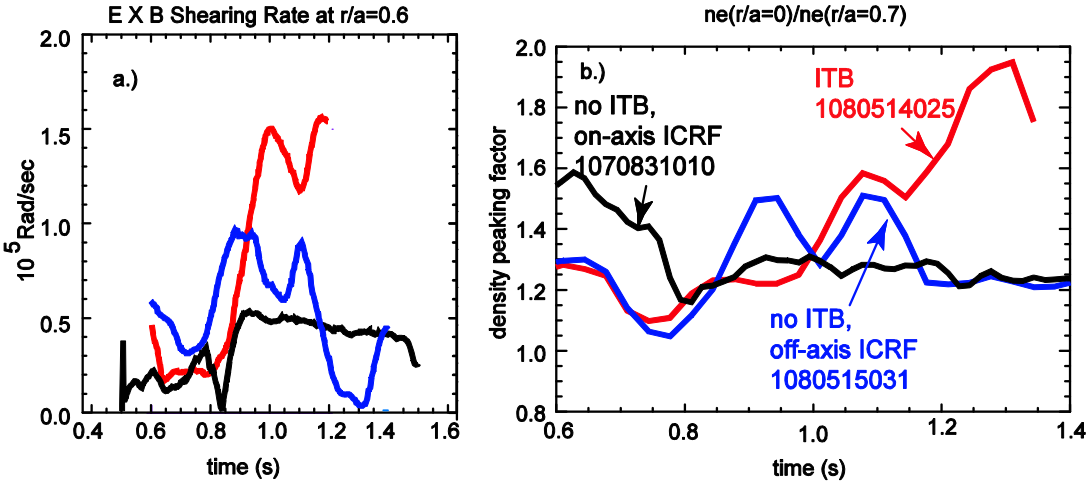

Fig. 11 Time history ofa.) EXB shearing rates at r/a=0.6 for off-axis ICRF heated EDA H-mode plasma with ITB (red) compared with off-axis ICRF heated EDA H-mode plasma with no ITB (blue) and with centrally ICRF heated H-mode no ITB (black) b.) density peaking for the same plasmas.

Measurement of the poloidal velocity profile is available in a small number of cases for ITB shots from the CXRS measurements of the boron impurities from r/a=0.3 outward. These data indicate that the poloidal velocity is near zero outside of the ITB region, but has a peak of +10 km/s at r/a=0.4 at the time that the ITB is established. Calculations of the radial electric field using both the toroidal and the poloidal velocity obtained from CXRS show a radial electric field well in the vicinity of the ITB foot (Fig. 12) [36]. Note that the electric field shown in this plot marked H-mode is taken at an earlier time slice in the same plasma after the H-mode transition and before the development of the ITB. That means that the ICRF heating is off-axis so the H-mode electric field profile (blue line) should be compared with that from the off-axis ICRF non-ITB discharges at the time immediately following the H-mode transition (black line in Fig. 9.b) rather than that of the centrally heated H-mode (Fig 8.a). It should also be noted that the data in Fig. 12 is taken from a different plasma from that in Fig 9. In addition, Fig. 12 incorporates both toroidal and poloidal velocity in the determination of the electric field while only toroidal rotation measurements were used to obtain the electric field shown in Fig. 9. These measurements have not yet been incorporated into the transport analysis. However, they suggest that the EXB shearing rate that will result

from calculations using these data will show even stronger shearing than what has already

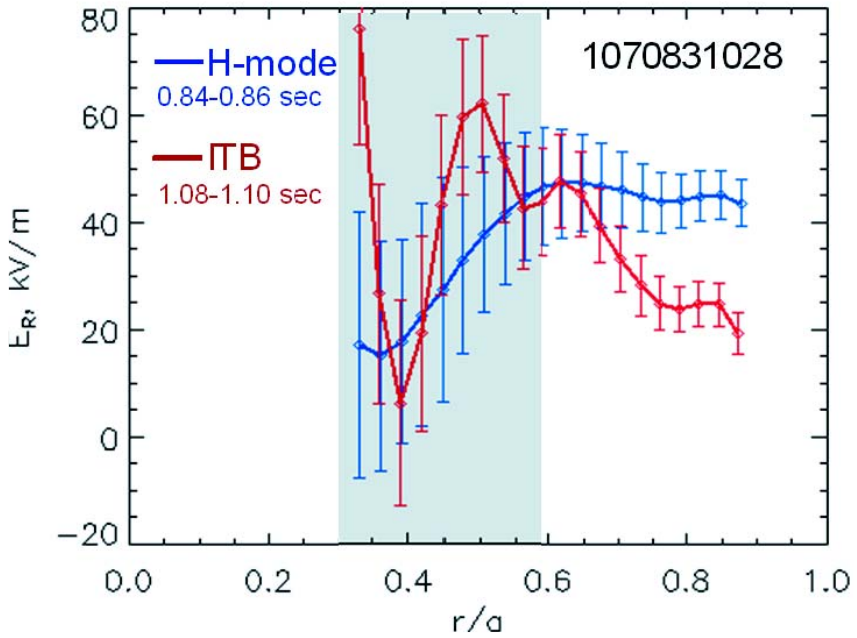

been reported.

Fig. 12 Radial electric field obtained from CXRS toroidal and poloidal rotation data for H-mode) blue and ITB (red) plasma. ICRF heating is off-axis for both.

V *Discussion*

For many of the toroidal experiments exhibiting ITB behavior cited earlier, it is thought that the rotation of the plasma that results from directed neutral beam deposition can generate sufficient electromagnetic shear to stabilize the ion temperature gradient driven instability (ITG) by increasing the E X B shearing rate above its maximum linear growth rate. Because there are no neutral beams or other external sources of momentum input to C-Mod, an explanation of the ITB formation that did not include the role of rotational shear was initially pursued. Several studies using both the linear and non-linear gyrokinetic code GS2 [39,40] to examine the ITG growth rate in C-Mod at the onset time of the ITB have been carried out. Using non-linear GS2 modeling, Redi *et al.* [27] found that a region of reduced turbulent

driven transport exists just inside the ITB foot. Linear GS2 modeling indicates that the ion temperature gradient mode has a finite growth rate at the barrier location at the onset time but is much smaller than is the strong growth rate found outside of the barrier where the density gradient is near zero.

Further analysis was done by Zhurovich [28] on plasmas that were part of a magnetic field scan, i.e. the ICRF resonance was moved shot by shot until ITBs began to form in the H-mode phase of the plasma. This study found that the region of the core plasma stable to ITG modes expanded in width as the ICRF resonance was moved further off-axis, resulting in the central zone of the plasma displaying no microturbulent driven outward flux. The neoclassical pinch is then strong enough to account for the density peaking in the core. The resulting growth rate profiles are shown in Fig. 13.

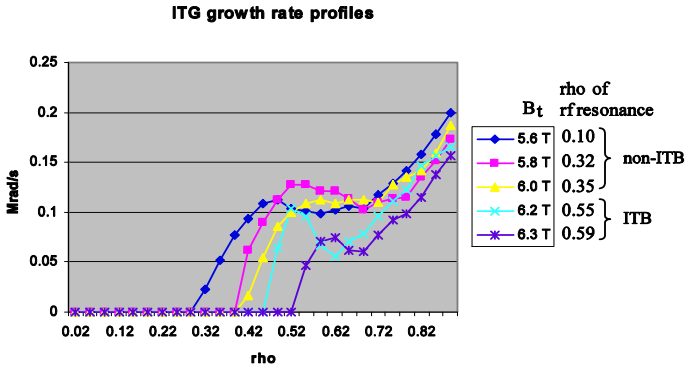

Figure 13. Linear ITG growth rate profiles calculated at ITB onset times. Higher field corresponds to more off-axis heating. There is no ITG turbulence in the core plasma region. The region of stability to ITG modes gets wider as the ICRF resonance is moved outward by changing the magnetic field. For ITB discharges it extends radially to approximately the location of ITB foot at r/a=0.5. ITG growth rates are systematically lower for the discharges that developed ITBs.

Thus the onset of ITBs in Alcator C-Mod has been explained by ion temperature profile modification caused by movement of the ICRF heating resonance well off-axis (it should be noted that because of the high density of C-Mod plasmas, the energy of the minority ion tail is only a few times higher than the central ion temperature, which allows equal power absorption by the majority ions and electrons in the plasma). This flattening of

the ion temperature gradient reduces the turbulent drive for the ion temperature. The question remains however, whether this is sufficient in light of the fact the rotational shear has been shown to play a strong role in other devices. The linear growth rates for ITG instability in both studies found growth rates of the order of 0.1 MRad/s in the barrier region. Despite the reduction of the growth rate with flattening of the ion temperature profile, the linear growth rate remains non-zero. It is possible that additional suppression of the instability is required.

In the previous section, it was determined that the intrinsic toroidal rotation profile that evolves during ITB plasmas results in an EXB shearing rate in the region $0.6 < r/a < 0.7$ of 1.5×10^5 rad/s. This rate exceeds the maximum growth rates for the ITG instability found in that region of similar plasmas in both of the two modeling studies cited above. The shearing rate found in the plasma with off-axis ICRF heating that did not form an ITB falls short of the maximum growth found in these studies and remains less than 1×10^5 radians/s. The time history of the shearing rate increase shows that it occurs well before the density peaking in the profile that is attributed to the ITB is seen. This indicates that the change in the toroidal rotation velocity is not caused by the change in the pressure profile and suggests that the rotation profile could also play a role suppressing ITG turbulence driven fluxes in C-Mod. Further study with gyrokinetic stability codes of the actual plasma conditions where these data are obtained is warranted.

VI. *Conclusion*

Alcator C-Mod is unique in displaying the presence of internal transport barrier development in H-mode plasmas with monotonic q-profiles ($q_{min} \leq 1$) without the introduction of external torque to the plasma. Despite the absence of neutral beams, an intrinsic rotation develops in all C-Mod plasmas, but is especially strong after the transition to H-Mode in the co-current

direction. In off-axis heated plasmas the core toroidal rotation decreases and often reverses direction soon after the H-mode transition while the rotation outside of the half radius shows little change. In plasmas where an ITB forms in such plasmas, this strong core rotation continues to decrease as the ITB density becomes more peaked. The hollow rotation profile results in the formation of a radial electric field well which in turn produces an EXB shearing rate that is significant in the region where the ITB foot is located. Comparison with gyrokinetic stability calculations from earlier ITB plasmas demonstrates that this shear has sufficient magnitude to suppress the ITG growth rate that would be expected in that region.

Acknowledgements

The authors are indebted to Manfred Bitter and Ken Hill of PPPL and Alex Ince-Cushman, formerly of MIT, for preparing the instrumentation for measurement of the toroidal rotation profiles. The transport analysis was aided by the work of David Mikkelsen and Doug McCune at PPPL, in helping the authors learn the proper use of the NCLASS package. The authors would also like to acknowledge the assistance and support of the C-Mod experimental staff.

References

[1]ASDEX Team, 1989 *Nucl. Fusion* **29** 1959

[2] Levinton F M *et al*1995 *Phys. Rev. Lett.* **75** 4417

[3]Strait E J *et al* 1995 *Phys. Rev. Lett.* **75** 4421

[4]Fujita T *et al* 1997 *Phys. Rev. Lett.* **78** 2377

[5]Gruber O *et al* 1999 *Phys. Rev. Lett.* **83** 1787

[6]Koide Y *et al* 1994 *Phys. Rev. Lett.* **72** 3662

[7] Synakowski E *et al.* 1997 *Phys Rev. Lett.* **78** 2972

[8] Burrell K H 1997 *Phys Plasmas* **4** 1499

[9]Sakamoto Y *et al.* 2001 *Nucl. Fusion* **41** 865

[10] de Vries P C *et al.* 2009 *Nucl. Fusion* **49** 075007

[11] Shafer M W *et al.* 2009 *Phys. Rev. Lett.* **103** 075004

[12] Ida K *et al.* 1998 *J. Phys. Soc. Jpn.* **67** 4089

[13] Nagashima K *et al.* 1994 *Nucl. Fusion* **34** 449

[14] Rice J E *et al* 1999 *Nucl. Fusion* **39** 1175

[15] Ernst D R *et al.* 1998 *Phys. Plasma* **5** 665

[16] deGrassie J S *et al.* 2004 *Phys. Plasma* **11** 4323

[17] Ida K *et al.* 2001 *Phys. Rev. Lett.* **86** 3040

[18]Pericoli Ridolfini V *et al* 2003 *Nucl. Fusion* **6** 469

[19]Lashkul S I *et al* 2000 *Plasma Phys. Control. Fusion* **42** A169

[20]Fujisawa A *et al* 1999 *Phys. Rev. Lett.* **82** 2669

[21]LeBlanc B *et al* 1995 *Phys. Plasmas* **2** 741

[22]Wolf R C 2003 *Plasma Phys, and Control. Fu*sion **45** R1

[23]Connor J W *et al* 2004 *Nucl. Fusion* **44** R1

[24]Fiore C L *et al* 2001 *Phys. Plasmas* **8** 2023

[25]Rice J E *et al* 2001 *Nucl. Fusion* **41** 277

[26]Lin L *et al*. 2009 *Phys. Plasmas* **16** 012502

[27]Redi M H *et al.* 2005 *Phys. Plasmas* **12** 072519-1

[28] K. Zhurovich *et al* 2007 *Nucl. Fusion* **47** 1220-1231

[29]Marmar E S *et al* 2001 Rev. Sci. Instrum.**72** 940

[30]Fiore C L *et al* 2004 *Plasma Phys. Control. Fusion* **46** B281

[31]Fiore C L *et al* 2007 *Fusion Science and Technology* **51** 303-316

[32]Fiore C L *et al* 2004 *Phys. Plasmas* **10** 2480

[33] Rice J E and Marmar E S 1995 *Rev. Sci. Instrum*. **66** 752

[34] Ince-Cushman A *et al* 2000 *Rev. Sci. Instrum.***79** 10F302

[35]Rice J E *et al* 2002 *Nucl. Fusion* **42** 510

[36]Rowan W L *et al* 2008 *Nucl. Fusion* **48** 105005

[37]Hawryluk R 1979 in *Physics of Plasma Close to Thermonuclear Conditions*

(Varennna,1979), Commission of the European Communities, Brussels, Vol. I p 61

[38]Houlberg W.A. *et al* 1997 *Phys. Plasmas* **4** 3230

[39] Kotschenreuther M *et al* 1995 *Comput. Phys. Commun.* **88** 129

[40]Dorland W *et al.* 2000 *Phys. Rev. Lett.* **85** 5579